Radiological Imaging

The Theory of Image Formation, Detection, and Processing

Volume 1

Harrison H. Barrett
William Swindell

Department of Radiology
and
Optical Sciences Center
University of Arizona
Tucson, Arizona

1981

ACADEMIC PRESS
A Subsidiary of Harcourt Brace Jovanovich, Publishers

New York London
Paris San Diego San Francisco
São Paulo Sydney Tokyo Toronto

5.3.1 Fundamentals of Intensifying Screens

There is a slight but nonnegligible radiation hazard associated with any x-ray examination of a living object. To minimize the risk, the detectors should be as efficient as possible, thus allowing the incident exposure levels to be as low as possible. A simple calculation shows that photographic film is intrinsically poor in this respect. A typical emulsion stops 1–2% of x-ray photons of energy 100 keV.

Detection efficiency is increased by one or two orders of magnitude if the film is placed in contact with a fluorescent phosphor screen. X rays are absorbed by the phosphor material, which then produces many photons, perhaps several thousand, with energies in the 1–5 eV range. These "optical" photons then expose the photographic film. Improved detector efficiency stems from two sources. First, the intrinsic x-ray photon absorption can be quite large because of the heavy metal ions in the phosphor and because the screen thickness is typically many times thicker than that of a photographic emulsion. Second, the optical photons created by the absorption of one x-ray photon will expose several grains in the emulsion.

The cross section of a typical screen is shown in Fig. 5.19. The support layer is made of cardboard or plastic and is stiff enough to discourage severe bending that would make the phosphor layer flake off. Between the phosphor and the support is a thin backing layer. Depending upon the application, this layer may contain diffusely reflecting white pigmentation to increase the light exposure on the film or it may contain an absorber in order to reduce light spreading and thus improve spatial resolution of the system. The active layer is made of phosphor particles of typical size 10 μ, bonded together with a binding agent. The layer thickness typically ranges between 70 and 280 μ. The binding agent may be transparent to enhance light output or an absorbing dye may be used to reduce the spread of light. The phosphor *packing fraction*, which is the fractional volume of the phosphor layer that actually contains active phosphor crystals, is typically 50%. On top is a protective transparent cover layer. Its thickness, typically 15 μ, is a compromise between providing adequate protection and keeping the spread of light between the film and the phosphor layer as small as possible.

The factors that increase the light output generally degrade the system resolution by increasing the spread of light photons at the photographic film. Light output is greater with thick screens (more x rays absorbed), transparent binder material, and a reflective under layer.

At diagnostic energy levels photoelectric absorption is the dominant primary x-ray interaction. Part of the primary energy is given up in ionizing the K or L shell of the absorbing atom, and the excess goes into the kinetic energy of the photoelectron. The excited ion will decay either by emitting fluorescent x radiation, which may or may not be reabsorbed in the screen, or by the emission of Auger electrons. The first product of the decay process is one or more relatively high-energy electrons moving in the lattice. High-speed electrons lose energy by inelastic collisions with other loosely bound (valence) electrons in the solid, creating energetic conduction-band electrons and leaving holes in the valence band. Little energy is communicated to the

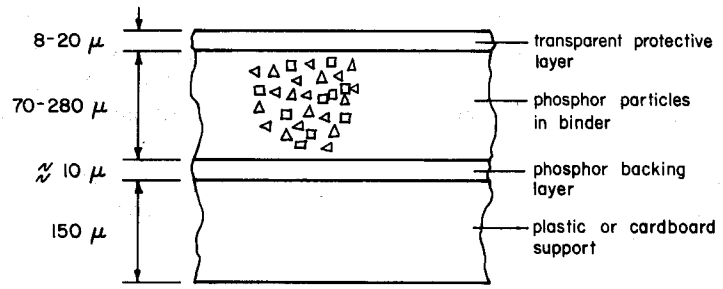

Fig. 5.19 Cross section of a phosphor screen used in clinical radiography. Dimensions shown are typical for commonly used systems.

lattice until the electron-hole energies are reduced to a much lower level of typically 12 eV. At these lower energies, electron–phonon interactions remove much of the remaining energy, generating heat and leaving each electron-hole pair with only the band-gap potential energy of typically 3 or 4 eV. Ultraviolet or optical photons will now be emitted as the electrons and holes recombine. This fluorescence may take place via an intermediate impurity level associated with small amounts of "activator" that are deliberately introduced into the lattice. This final step of the decay process is often quite efficient. As many as 90% of the conduction-band electrons may decay with the emission of an optical photon. With impurity-activated scintillators there are additional losses. For example, in sodium-activated cesium iodide only about half of the cesium iodide band-gap energy is converted during the optical fluorescent decay. Figure 5.20 summarizes the chain of events. Several parameters are needed to describe the efficiency of the conversion process. The optical gain factor m is defined by

$$m = \frac{\text{number of optical photons liberated}}{\text{number of absorbed primary x-ray photons}}. \tag{5.118}$$

The stopping power of the screen η_1 is simply the fractional number of x-ray photons that are absorbed by the screen:

$$\eta_1 = \frac{\text{number of x-ray photons absorbed by screen}}{\text{number of x-ray photons incident on screen}}. \tag{5.119}$$

The intrinsic efficiency of the phosphor η_2 is defined as the ratio of the energy of the emitted optical photons to the energy of the primary x ray, $\mathscr{E}_x$.

$$\eta_2 = \frac{m\mathscr{E}_o}{\mathscr{E}_x}, \tag{5.120}$$

where $\mathscr{E}_o$ is the energy associated with one optical photon. Some fraction α of the optical energy escapes the screen, and the screen efficiency η_3 is defined by

$$\eta_3 = \alpha\eta_2. \tag{5.121}$$

For most screens α is about 0.5.

The large loss of energy to thermal excitation seems inescapable, and the present maximum values of screen efficiency of around 25% are unlikely to be significantly improved upon. The commonly used calcium tungstate scintillator has an intrinsic efficiency of about 5%. As an example, we can calculate the approximate number of optical photons ($\sim$3 eV) emitted from a calcium tungstate screen for each absorbed 100 keV primary x ray:

$$\text{number of emitted optical photons} \approx \frac{100\text{ keV}}{3\text{ eV}} \times 5\% \times 0.5 \approx 800. \tag{5.122}$$

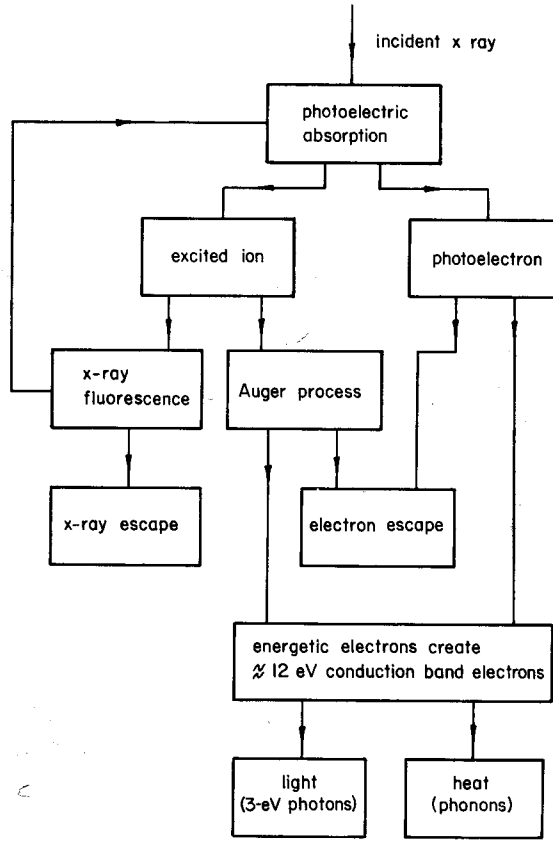

Fig. 5.20 Chain of events relating to the production of low-energy (~3 eV) photons starting with the absorption of a high-energy x ray in a phosphor material. Compton events are not shown.

5.3.2 Use of Screens

Most x-ray film has light-sensitive emulsion coated onto both sides. The normal practice is to sandwich such film between two fluorescent intensifying screens in a light-tight cassette. Foam rubber pads, or similar devices, ensure that the screens and film make intimate contact, thus preventing degradation of spatial resolution in the final image. Essentially all of the film exposure is caused by fluroescent optical radiation from the screens. Very little exposure can be attributed to the direct interaction of x rays with the photographic

emulsion. It is common practice to use front and rear screens of the same thickness. However, in order to equalize the light exposure from the two screens, a thinner front screen is sometimes used.

Using a thinner front screen also tends to equalize the point spread functions of the two screens. If the screens are of equal thickness, the differential absorption of x rays as the beam traverses the system results in the average distance between the point of absorption in the screen and the emulsion being greater for the front screen. Thus there is more spreading of light from the front screen of a pair of equal thickness.

Resolution is degraded by "crossover," the exposure of an emulsion by optical photons that have crossed through the film base. Diffusion and scattering in the intervening emulsion produces unwanted blur in the crossover components of the final exposure. The effect is minimized by using ultraviolet-emitting screens since ultraviolet radiation is strongly absorbed by the film base material. Blue and (especially) green light is less strongly absorbed, and screens emitting these wavelengths will produce a less sharp image, other things being equal.

When high resolution is required, a single-emulsion film and a single screen may be used. The ultimate detail in the x-ray image is obtained by using no screen at all. In this case, special thick emulsions are employed in order to recoup some of the lost system sensitivity. In order to realize this ultimate resolution, careful attention must also be paid to other factors such as source size, patient motion, scattered radiation, etc.

There is a wide range in speed for commercially available screens. The fastest ones are thicker and have poorer resolution; they also show more "mottle" (see Sections 5.3.4 and 10.4). They are used whenever dose reduction is important. They may also be used when the object is low contrast and poorly defined in the first place. These high-speed screens can also prevent image blurring due to patient motion. On the other hand, high-resolution imaging requires that the screens be thin and necessarily slower, so there is an increased dose to the patient. Much of the skill of the radiologist is concerned with choosing the optimum combination of beam filter, beam energy, screen type, and film for a particular clinical examination.

For over 70 years, calcium tungstate has been the most used phosphor. It has excellent mechanical properties and an emission spectrum in the blue and ultraviolet that is ideal for exposing photographic emulsions. Over the past few years new phosphors have been introduced in an attempt to reduce the exposure given to the patient. These new phosphors fall into two main classes: the green-emitting rare-earth oxysulphides (terbium activated) X_2O_2S:Tb, where X is gadolinium, lanthanum, or yttrium, and the blue- and ultraviolet-emitting phosphors such as lanthanum oxybromide LaOBr:

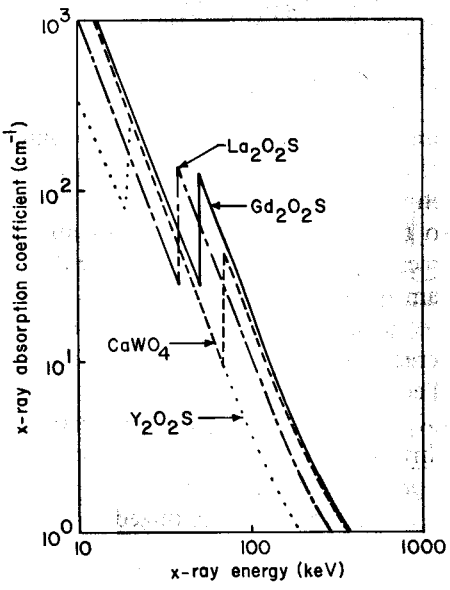

Fig. 5.21 X-ray absorption coefficient for commonly used phosphor materials.

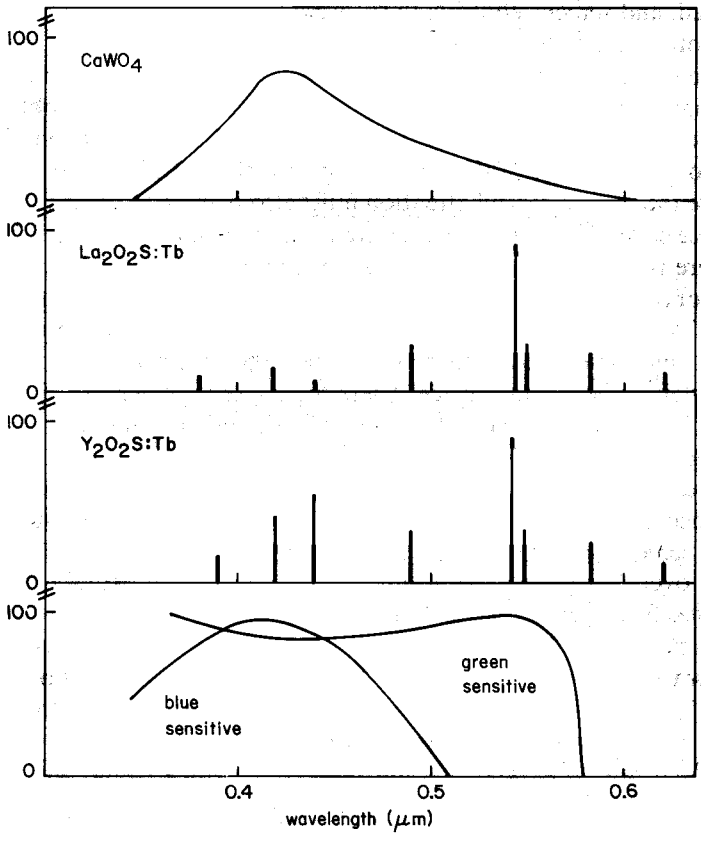

Fig. 5.22 Emission spectra of three commonly used phosphors and the spectral response of blue- and green-sensitive film. Calcium tungstate has a broad emission band which matches blue- and ultraviolet-sensitive emulsions. The line spectra of the rare-earth scintillators require film with extended green response for optimum matching. The length of the lines gives an indication of the relative line strengths.

Tm and barium fluorochloride BaFCl:Eu. The spectral properties of these materials are shown in Figs. 5.21 and 5.22.

5.3.3 Large-Area Optical Properties

The large-area property of interest here is the relationship between film density and the incident x-ray exposure. This characteristic is equivalent to the H–D curve for a photographic emulsion when exposed to light. Indeed, the shape of the curve for the film-screen combination is determined almost entirely by the H–D curve of the film itself since every operation leading to the generation of optical photons is linear with respect to the incident x-ray exposure. In order to define the speed of the system, it is necessary to clearly define the conditions under which a speed measurement is made. A commonly used speed index is determined from the x-ray exposure in roentgens required to blacken the film to a density of 1.0 above the base and fog level. The x-ray beam quality, as determined by the accelerating voltage and added filtration, must be specified. To be rigorous, the type of power supply and rectification and the target material should also be included. It is common to compare systems by stating the *relative* speeds or relative exposure factors (which are given by the reciprocals of the relative speeds).

In addition to the speed of the film itself, there are four distinct processes that combine to determine the overall speed of the system. They are the absorption of x rays by the phosphor, the emission of fluorescent radiation by the phosphor, the efficiency with which these photons are coupled to the emulsion, and the spectral response of the film. These factors are discussed in more detail in the next paragraphs.

The absorption of x rays is determined by the mass absorption coefficient of the phosphor $(\mu(\mathscr{E})/\rho)$, the spectral density $\Phi_{\mathscr{E}}(\mathscr{E})$ of the incident x-ray fluence, and the coating weight of the phosphor W. Nearly all of the primary beam attenuation is by photoelectric absorption within the phosphor material, so the efficiency η_1 of the first stage [see (5.119)] is given approximately by

$$\eta_1 = \frac{\int_0^\infty [1 - \exp\{-W(\mu(\mathscr{E})/\rho)\}]\Phi_{\mathscr{E}}(\mathscr{E})\,d\mathscr{E}}{\int_0^\infty \Phi_{\mathscr{E}}(\mathscr{E})\,d\mathscr{E}}. \tag{5.123}$$

Note that the denominator in (5.123) is simply the total incident x-ray fluence Φ. The coating weight W is related to the actual screen thickness d_1 by

$$W = d_1 \rho f, \tag{5.124}$$

where ρ is the density of the phosphor material and f is the packing fraction. Clearly, η_1 can be made close to unity by having a thick enough screen. However, an unduly thick screen compromises other desirable system features. Thickness is the single most important parameter in controlling the speed-resolution trade-off. Efficiency η_1 is also affected by the presence of K-absorption edges lying within the source spectrum. Consider two beams of monochromatic x rays impinging upon a Gd_2O_2S screen with energies just straddling the K-absorption edge of gadolinium. For a typical screen thickness of 100 μm with a packing fraction of 50%, the ratio of stopping powers is given by $\{1 - \exp[-(0.01 \times 0.5 \times 130)]\}/\{1 - \exp[-(0.01 \times 0.5 \times 25)]\} \approx 4$. (see Fig. 5.21 for the values of μ). For the more energetic primary beam, much of the absorbed energy is reradiated, without capture, by K-shell fluorescence and is lost to the energy conversion process. Nearly all of the energy of the less energetic beam is imparted to the photoelectron and therefore is available for conversion to light. Thus screen efficiency is higher for the more energetic beam but not by the factor predicted above. The fraction lost by K escape is reduced as the screen thickness increases (see Figs. 5.23–5.25 and Table 5.2).

The conversion efficiency η_2, defined as the optical energy output as a fraction of the x-ray energy absorbed, is determined by the type of phosphor material. For calcium tungstate this figure is quite low, in the region of 5%. For the rare-earth oxysulphide screens, the figure is higher at 13% (lanthanum) and 18% (gadolinium). The highest achieved efficiency is 25% using

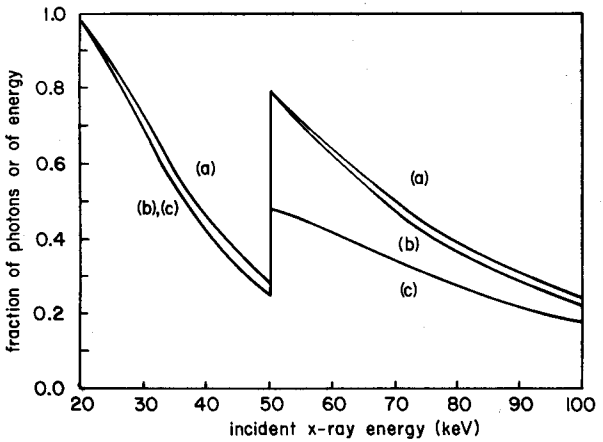

Fig. 5.23 Interaction of x-ray photons with a pair of Alpha-8 (3M) screens containing 0.105 g/cm^2 Gd_2O_2S. (a) Total stopping power in fractional number of incident photons interacting with the screen. (b) Fraction stopped due just to photoelectric interactions. (c) Fraction of the incident energy deposited in the screen. Above the gadolinium K-absorption edge, a significant amount of energy is lost due to the escape of K_α radiation. (From Venema, 1979.)

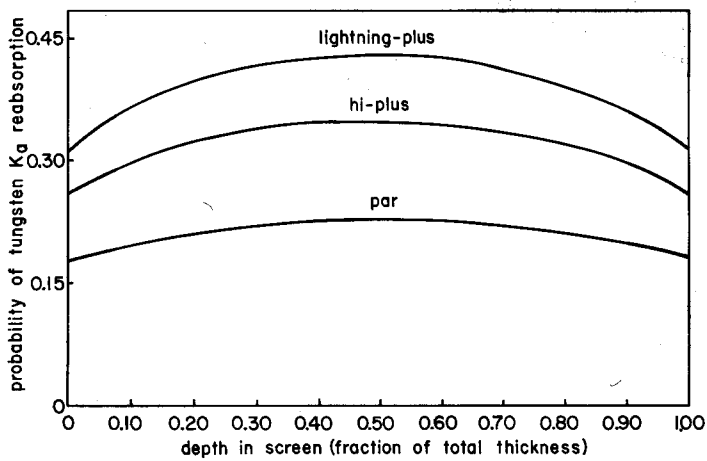

Fig. 5.24 Probability of reabsorption of fluorescent K_α radiation increases with increasing screen thickness and is slightly higher for x rays originating near the center of the screen. These figures of calculated probabilities are taken from Vyborny *et al.* (1978).

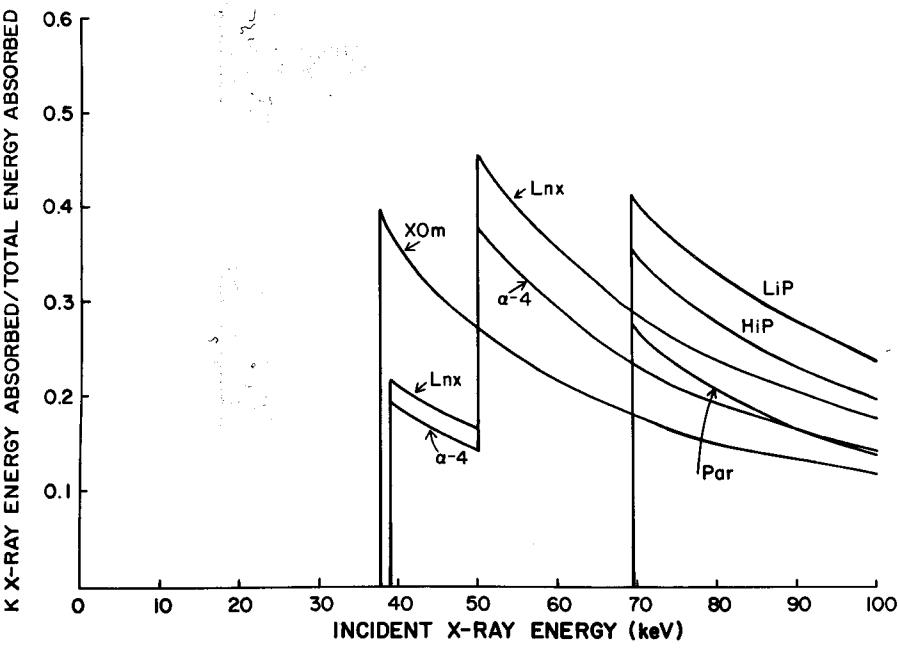

Fig. 5.25 Fraction of the total deposited energy that is due to reabsorbed fluorescent radiation in various screens: XOm, X-Omatic; α-4, Alpha-4; Lnx, Lanex Regular; LiP, Lightning-Plus; HiP, High-Plus; and Par. (From Vyborny *et al.*, 1978.)

TABLE 5.2

Screens[a]

Group	Brand	Manufacturer	Phosphor	Highest atomic number	*K*-absorption edge (KeV)	Color of fluorescent light	Phosphor mass (mg/cm^2)	$P_{esc}(\%)$
I	Universal	Auer	$CaWO_4$	74	69.5	Blue	96	75
I	Spezial	Siemens	$CaWO_4$	74	69.5	Blue	132	69
II	Alpha-8	3M	Gd_2O_2S:Tb	64	50.2	Blue + green	105	60
II	Lanex-Regular	Kodak	Gd_2O_2S:Tb /La_2O_2S:Tb	64/57	50.2/38.9	Blue + green	125/9	50/38
III	MR 600	Agfa-Gevaert	LaOBr:Tb	57/35	38.9/13.5	Mainly Blue	128	40
III	MR 400	Agfa-Gevaert	LaOBr:Tb	57/35	38.9/13.5	Mainly Blue	87	4/48
III	Rapide	Ilford	LaOBr:Tb	57/35	38.9/13.5	Mainly Blue	82	5/50
III	Quanta II	DuPont	$BaFCl:Eu^{2+}$	56	37.4	Blue	86	5/56
IV	Rarex-B	Radelin	Y_2O_2S:Tb	39	17.0	Mainly Blue	116	34 (24 at high energy)

[a] Physical characteristics of some commercially available screens. The escaping photon fraction $P_{esc}(\%)$ varies less than 1% with energy change above the *K* edge except where noted. Adapted from Venema (1979).

silver-doped zinc sulphide screens. It seems unlikely that significant improvements in this area will be realized. Nor are they really needed since, as we shall see, the major and fundamental limitation to overall improvement of diagnostic x-ray imaging systems is the quantum noise associated with the detection of incident x rays.

Optical coupling to the film is governed by scattering in the phosphor-binder complex, reflection losses at the phosphor-film interface, absorption in the phosphor layer, and absorption by the film emulsion. High-resolution screens have absorbing dye in the binder to reduce light spreading. In these screens, there is an optimum thickness for maximum optical efficiency. In the front screen, more light will be generated near the entrance face, away from the film, than will be generated near the film. Optical absorption losses will absorb the stronger optical flux before it reaches the screen. For low x-ray energies where the x-ray beam is rapidly attenuated near the entrance face, a significant fraction of the optical radiation may not reach the film.

Some of the newer phosphors emit significant amounts of energy in the green part of the spectrum (see Fig. 5.22). Special green-sensitive films are needed to take full advantage of this characteristic. Other new phosphors emit efficiently in the blue and ultraviolet regions and special film types are not needed to utilize the enhanced efficiency.

It is the combination of all these effects that determines the overall speed and variation of speed with beam quality. Data representative of commercially available screens and films are shown in Table 5.3a and b.

5.3.4 Noise and Resolution Overview

We now look qualitatively at how the imaging properties of a film–screen system depend upon its physical properties.

In the film–screen system the PSF is determined almost entirely by the diffusion of light inside the phosphor screen. The photographic emulsion is too thin to contribute any significant additional spreading to the bunch of optical photons generated within the phosphor. A detailed calculation of the PSF will involve calculating the light distribution at the film for a fluorescent event at a given location in the screen and then integrating this result over the depth of the screen. Appropriate weighting factors for variation of x-ray flux with depth and absorption of light by any dyes present must be applied (see Fig. 5.26).

The ability to record fine detail in the object may be limited by noise, rather than geometrical considerations. Consider a phosphor screen that has a relatively low optical conversion efficiency. In order to expose the film and yield a net density of (for example) 1.0, a relatively high incident

TABLE 5.3a

Relative Speed of Several Film–Screen Combinations for Blue-Sensitive Film[a]

Screen	Manufacturer	Phosphor	Dye	Relative speed for film type[b]			
				I	II	III	IV
Detail	DuPont	$CaWO_4$	Yellow	0.1	0.2	0.3	0.4
X-Omatic Fine	Kodak	$BaSrSO_4$	Yellow	0.15	0.3	0.45	0.6
Fast Detail	DuPont	$CaWO_4$	None	0.2	0.4	0.6	0.8
Par	DuPont	$CaWO_4$	None	0.4	0.8	1.2	1.6
Rarex BG Detail	U.S. Radium	75% Gd_2O_2S:Tb; 25% Y_2O_2S:Tb	—	0.5	1.0	1.5	2.0
Hi-Speed	DuPont	$BaPbSO_4$	—	0.6	1.2	1.8	2.4
Hi-Plus	DuPont	$CaWO_4$	None	0.8	1.6	2.4	3.2
X-Omatic Regular	Kodak	$BaSrSO_4$	Yellow	0.8	1.6	2.4	3.2
Rarex BG Mid-Speed	U.S. Radium	75% Gd_2O_2S:Tb; 25% Y_2O_2S:Tb	—	1.0	2.0	3.0	4.0
Blue Max 1	General Electric	LaOBr	—	1.0	2.0	3.0	4.0
Lightning Plus	DuPont	$CaWO_4$	None	1.2	2.4	3.6	4.8
Quanta II	DuPont	BaFCl	None	1.6	3.2	4.8	6.4
Rarex BG Hi-Speed	U.S. Radium	75% Gd_2O_2S:Tb; 25% Y_2O_2S:Tb	—	2.0	4.0	6.0	8.0
Blue Max 2	General Electric	LaOBr	—	2.0	4.0	6.0	8.0

[a] Adapted from Rao *et al.* (1978).

[b] Numbers represent relative speeds of the stated combination. They may also be interpreted as the reciprocal of the approximate exposure (mR^{-1}) at 80 kVp with 35 mm of aluminium filtration required to produce a film density of 1.0 above fog level. The film types in each category are: I. Kodak XG, DuPont Cronex 7; II, Kodak XRP, DuPont Cronex 4, DuPont Cronex 6, DuPont Cronex 6+; III. Kodak XS; IV. Kodak XR.

TABLE 5.3b

Relative Speed of Several Film–Screen Combinations for Green-Sensitive Film[a]

Screen	Manufacturer	Phosphor	Dye	Relative speed for film type[b]		
				Kodak Ortho-G	3M XD	3M XM
Lanex Fine	Kodak	La_2O_2S:Tb Gd_2O_2S:Tb	None	1.0	1.3	3.3
Alpha 4	3M	La_2O_2S:Tb Gd_2O_2S:Tb	Pink	1.5	2.0	5.0
Alpha 8	3M	La_2O_2S:Tb Gd_2O_2S:Tb	None	3.0	4.0	10.0
Lanex Regular	Kodak	La_2O_2S:Tb Gd_2O_2S:Tb	None	3.5	4.7	11.7

[a] Adapted from Rao *et al.* (1978).
[b] See Table 5.3a, footnote *b*.

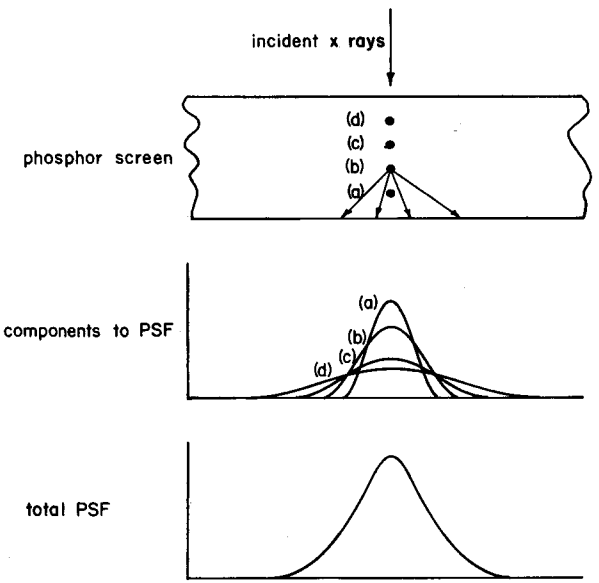

Fig. 5.26 How the point spread function of a phosphor screen is determined by integrating contributions from individual layers (a), (b), (c), (d).

x-ray fluence (photons per square centimeter) will be required. Next, consider a screen of higher optical conversion efficiency. Fewer x-ray photons per square centimeter will be required to yield a final net density of 1.0. If this latter system has a sufficiently high optical conversion efficiency, then the average spacing between incident x-ray quanta will become larger than the characteristic dimension of the PSF, and the film will no longer appear uniformly dense, but will have a "mottled" appearance. This phenomenon, called *quantum mottle*, is illustrated in Fig. 5.27. It is important to realize that these fluctuations are a direct result of the discrete nature of the detected x-ray photons. Quantum mottle can be seen when the widths of the component PSFs are comparable to or smaller than the mean spacing between incoming detected x rays. The mottled appearance detracts from the observer's ability to detect any small-scale and small-density fluctuations arising from real variations in the object that would otherwise have shown in the final image.

The nature of the trade-off involving overall speed, quantum mottle, and resolution is quite complicated, and until a quantitative basis for describing

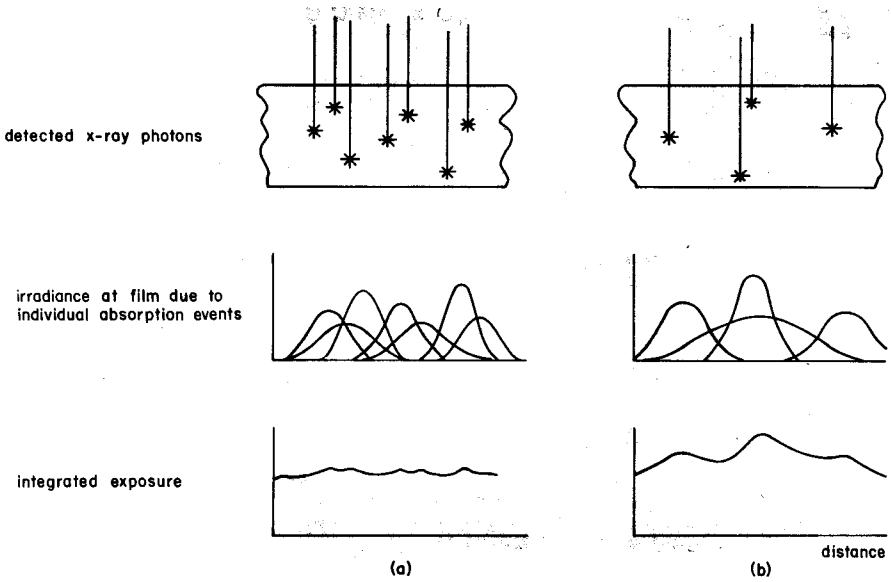

Fig. 5.27 Quantum mottle: (a) For a screen with low optical conversion efficiency, the individual light flashes from the detected x-ray photons add up to give a uniform exposure at the photographic film. (b) With a higher conversion efficiency, fewer detected x rays are needed to achieve the same average exposure level. Consequently, the wider average distance between the absorption events results in fluctuations in the mean exposure level, giving rise to a mottled appearance in the developed film.

TABLE 5.4

Principal Interactions among the FWHM of the Point Spread Function, Amount of Quantum Mottle, and Features That Determine the Overall Speed of the Film–Screen System

Method of increasing overall system speed[a]	Resultant change in amount of quantum mottle	Resultant change in FWHM of PSF
Increase film speed	Increase	No change
Increase optical conversion efficiency	Increase	No change
Increase screen thickness	Debatable	Increase
Increase phosphor absorption coefficient	No change	No change

[a] All other variables are held constant.

quantum mottle is established (Section 10.4), only qualitative statements can be made. The major interactions can be understood by considering a given system and then inquiring about the change in quantum noise (mottle) and minimum resolvable distance δ as the system speed is increased. There are basically four ways to increase the speed of the system (see Table 5.4). In all cases, increasing the system speed requires fewer incident x-ray photons per square centimeter, and mottle will increase as the mean spacing between detected x rays decreases. Only in the case of using a thicker screen is it debatable that the amount of mottle will increase since the larger component PSFs will smooth out the spatial distribution of film exposure even though fewer x-ray quanta are used. Of the variables included, the system resolution depends on only the thickness of the phosphor layer.

5.3.5 Point Spread Function—A Calculation

Since the PSF of the film–screen combination is determined almost entirely by the characteristics of the screen, it is convenient to neglect the film and simply work with the distribution of actinic radiation at the exit surface of the screen. We shall assume that the film receives a negligible amount of direct x-ray exposure compared to the exposure it receives from the fluorescent radiation, which is a reasonable assumption for practical purposes. One advantage in analyzing just the screen is that the inherent nonlinear characteristics of the film are not brought into consideration.

In keeping with the philosophy used elsewhere in the book, we shall use a simple model to illustrate the underlying principles. It will be seen that

even the simple model predicts a behavior that is remarkably close to that which is actually observed.

The model assumes that the screen, of total thickness d_s, is composed of a phosphor layer of thickness d_1 and a transparent cover layer of thickness d_2. The phosphor layer is assumed to be optically transparent with a non-reflecting front surface. The geometry is defined in Fig. 5.28. Quantity $\Phi_x(x, y)$ is the x-ray photon fluence (photons/cm^2) arriving at the screen. The problem is to calculate the optical fluence $\Phi_o(x, y)$ (photons/cm^2) in the plane of the emulsion for different distributions of $\Phi_x(x, y)$.

We begin by considering a volume element $dV = dx'\, dy'\, dz$ of the phosphor material located at $P_1(x', y', z)$ and calculating its contribution to the optical fluence at some point $P_2(x, y, d_s)$ in the plane of the emulsion.

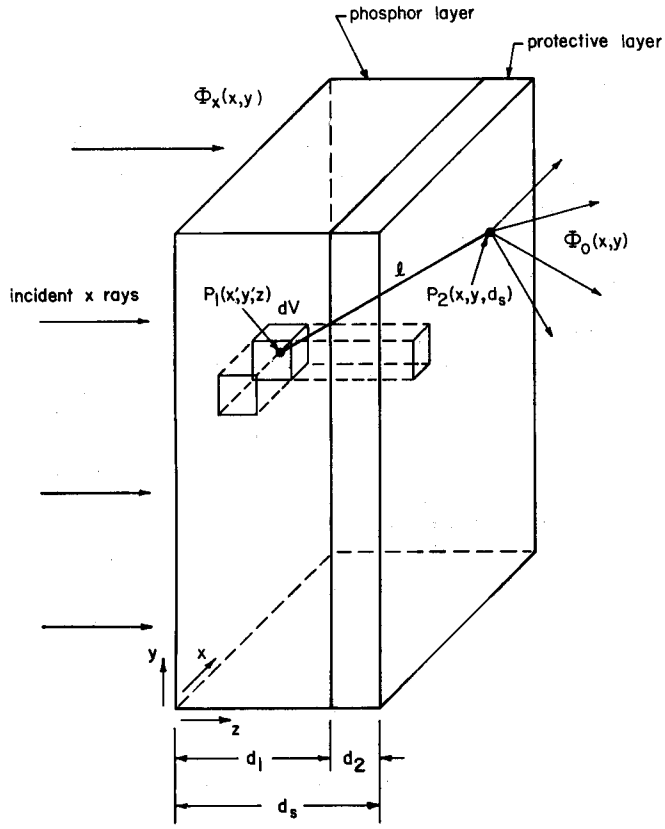

Fig. 5.28 Geometry used for calculating optical fluence $\Phi_0(x, y)$ (photons per square centimeter) at point P_2 in the exit plane of screen due to incoming x-ray fluence $\Phi_x(x, y)$.

The mean number of optical photons dN emitted from the volume element is given by

$$dN = \Phi_x(x', y')[\exp(-\mu z)]m\mu\, dx'\, dy'\, dz, \tag{5.125}$$

where m is the mean number of optical photons emitted per absorbed x-ray photon, $\exp(-\mu z)$ represents the attenuation of the primary beam before reaching the volume element, and $\mu\, dz$ represents the probability of absorption of an x-ray photon in traversing the element.

The contribution to the average optical fluence Φ_o at P_2 is given by

$$d\Phi_o(x, y) = \frac{dN}{4\pi}\frac{\cos\theta}{l^2},$$
$$l^2 = (x - x')^2 + (y - y')^2 + (d_s - z)^2, \tag{5.126}$$

where it is assumed that the optical photons are emitted at the point of absorption with an isotropic distribution over 4π steradians. The cosine term is the required obliquity factor, with θ being the angle between the normal to the screen surface and the direction of the incoming optical photon. By combining the two previous equations and integrating over the volume of the screen, we obtain a general expression for the optical fluence $\Phi_o(x, y)$ resulting from a general distribution of incident x-ray photon fluence $\Phi_x(x, y)$:

$$\Phi_o(x, y) = \frac{\mu m}{4\pi}\int_{-\infty}^{\infty}\int_{-\infty}^{\infty}\Phi_x(x', y')\, dx'\, dy'\int_0^{a_1}\frac{\exp(-\mu z)\cos\theta}{l^2}\, dz. \tag{5.127}$$

Strictly speaking, the limits of integration should be over the volume of the screen, but it is convenient and reasonable to use $\pm\infty$ for the x' and y' integration.

We now use this expression to calculate the point spread function of the screen. For this calculation, the input fluence $\Phi_x(x, y)$ is described by a delta distribution $\Phi_x^\delta(x, y)$, located at the origin for convenience, and defined by

$$\Phi_x^\delta(x, y) = \delta(x)\,\delta(y). \tag{5.128}$$

The point spread function is generally defined as the system output for a unit impulse at the input, so we shall note that the resulting expression for the PSF describes the optical fluence for one absorption event that is averaged over the phosphor thickness. This is not the same as the point spread function that would actually be observed due to a single isolated scintillation. There are two reasons for this. First, there are random fluctuations in both m, the number of optical photons, and the directions in which they are emitted, and second, the single event does not involve the integration over z that is shown in (5.127).

Using (5.127) and (5.128), we find an expression for the point spread function $p(x, y)$:

$$p(x, y) = \frac{\mu m}{4\pi} \int_0^{d_1} \frac{\exp(-\mu z)\cos\theta}{x^2 + y^2 + (d_s - z)^2}\, dz. \tag{5.129}$$

To obtain an analytical solution, we make the additional assumption that the probability of an x-ray photon being absorbed is a constant independent of penetration depth in the screen. This will happen when d_1 is sufficiently small that the term $\exp(-\mu z)$ can be replaced by unity for all z.

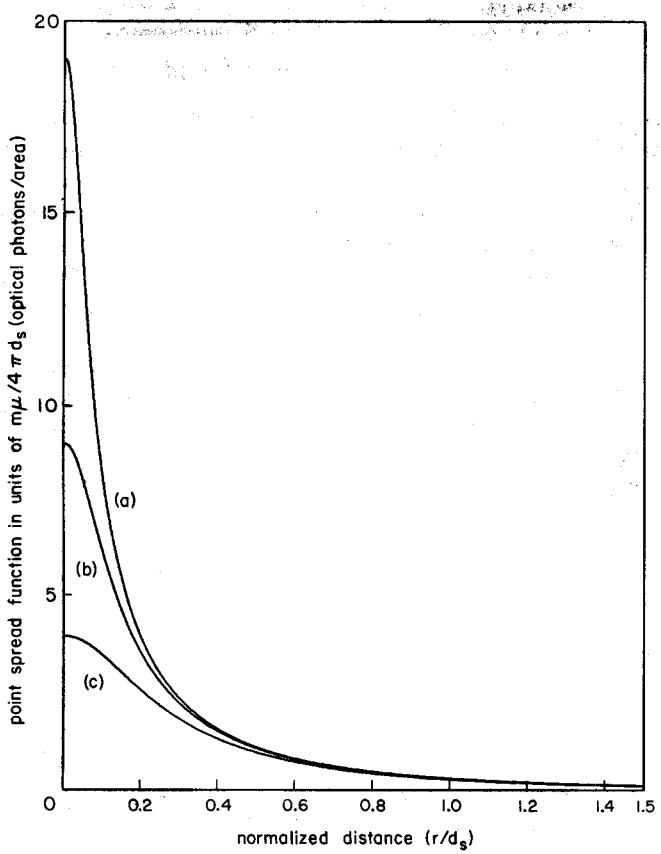

Fig. 5.29 Point spread function [see (5.131)] for a simple nonabsorbing, nonscattering screen for various thicknesses d_2 of the cover layer. The abscissa is normalized to d_s, the combined thickness of the phosphor layer and cover layer. Values of d_2/d_s are (a) 0.05, (b) 0.1, and (c) 0.2.

The final expression is

$$p(x, y) = \frac{\mu m}{4\pi} \int_0^{d_1} \frac{(d_s - z)}{[x^2 + y^2 + (d_s - z)^2]^{3/2}}\, dz. \tag{5.130}$$

This is a standard integral with solution

$$p(x, y) = \frac{\mu m}{4\pi} \left(\frac{1}{(r^2 + d_2^2)^{1/2}} - \frac{1}{(r^2 + d_s^2)^{1/2}} \right), \tag{5.131}$$

where $r^2 = x^2 + y^2$. This function is plotted in Fig. 5.29, where it is seen that the peak optical irradiance is strongly dependent upon the thickness of the protective layer relative to that of the phosphor layer. However, for distances from the center that are greater than about half the phosphor layer thickness, the optical flux density is almost independent of this relative thickness. The central part of the PSF does not influence the MTF of the screen too strongly however, as we shall soon see, because most of optical energy is distributed in the wings. The reader may verify that

$$\int_{-\infty}^{\infty} \int p(x, y)\, dx\, dy = 0.5 \mu m d_1 \tag{5.132}$$

and show that the right-hand side of (5.132) is exactly equal to half the mean number of optical photons that are generated in the phosphor layer per incident x-ray photon.

5.3.6 Line Spread Function

To calculate the line spread function, we go back to (5.127) and substitute for $\Phi_x(x, y)$ a line delta function distribution $\Phi_x^{\text{line}}(y)$ defined by

$$\Phi_x^{\text{line}}(y) = \delta(y). \tag{5.133}$$

This line source is distributed along the x axis. The substitution of (5.133) into (5.127) gives an expression for the line spread function $l(y)$:

$$l(y) = \frac{\mu m}{4} \int_{-\infty}^{\infty} \int_0^{d_1} \frac{(d_s - z)\, dx'\, dz}{[x'^2 + y^2 + (z - d_s)^2]^{3/2}}. \tag{5.134}$$

The double integration is straightforward, and we find that

$$l(y) = \frac{\mu m}{4\pi} \ln\left(\frac{y^2 + d_s^2}{y^2 + d_2^2} \right). \tag{5.135}$$

This quantity is plotted in Fig. 5.30.

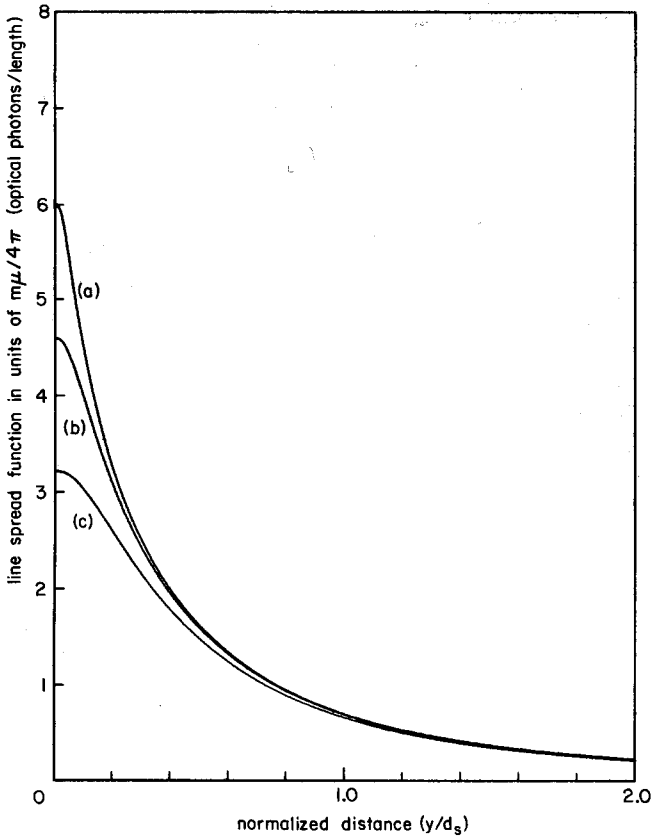

Fig. 5.30 Line spread function for simple nonabsorbing, nonscattering screen for various thicknesses d_2 of the cover layer. The abscissa is normalized to d_s, the combined thickness of phosphor layer and cover layer. Values of d_2/d_s are (a) 0.05, (b) 0.1, and (c) 0.2.

5.3.7 Modulation Transfer Function—A Calculation

Because of the circular symmetry, the screen transfer function may be described by a one-dimensional function $L(\eta)$ [see (2.101)], where $L(\eta)$ is obtained by taking the one-dimensional Fourier transform of $l(y)$:

$$L(\eta) = \frac{\mu m}{4\pi} \frac{[\exp(-2\pi\eta d_2) - \exp(-2\pi\eta d_s)]}{\eta}. \tag{5.136}$$

The modulation transfer function is then given by normalizing (5.136) to unity at $\eta = 0$:

$$\mathrm{MTF}(\eta) = \frac{\exp(-2\pi\eta d_2)[1 - \exp(-2\pi\eta d_1)]}{2\pi\eta d_1}, \tag{5.137}$$

where we have used $d_1 + d_2 = d_s$. This function is plotted in Fig. 5.31. It is evident that the MTF of a screen falls off rapidly with increasing frequency. The frequency content of the incident x-ray photon distribution must be limited to one cycle per two or three screen thicknesses in order for the optical image to contain a reasonable fraction of all frequency components present.

We close this section by showing that similar results follow from using more realistic models [see Swank (1973b) and Fig. 5.32]. One point to notice

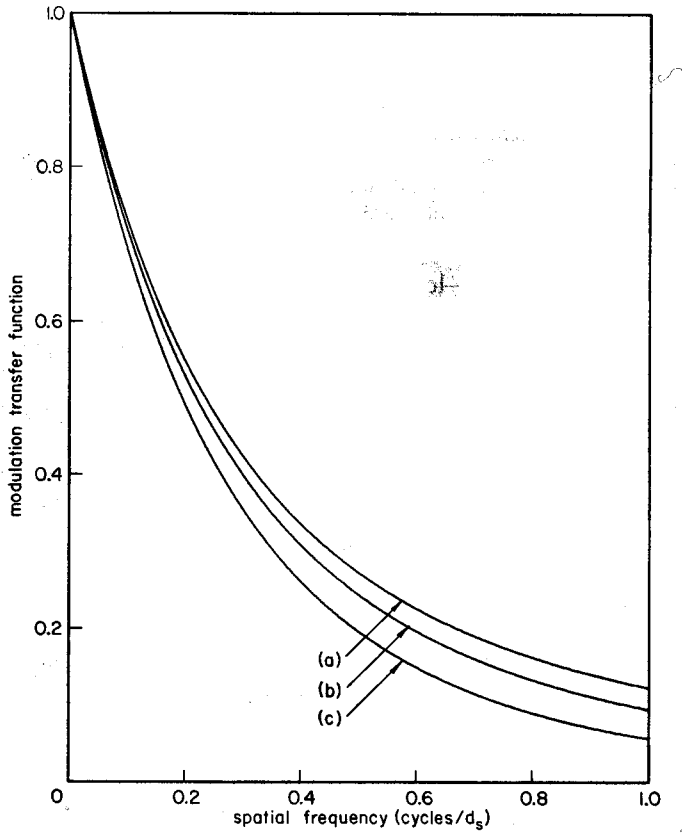

Fig. 5.31 Modulation transfer function of a simple nonabsorbing screen for various thicknesses d_2 of the cover layer as a function of normalized spatial frequency ηd_s, where d_s is the combined thickness of the phosphor layer and cover layer. Values of d_2/d_s are (a) 0.05, (b) 0.1, and (c) 0.2.

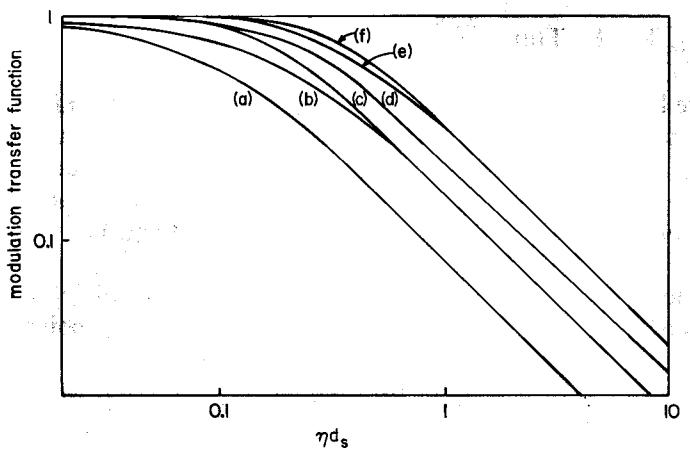

Fig. 5.32 Theoretical MTF for various screen models with screen thickness d_s: (a) transparent phosphor, reflective backing; (b) transparent phosphor, black backing; (c) scattering in the diffusion limit, no dyes reflective backing; (d) nonscattering, absorbing phosphor, reflective backing, 32% of light reaching output plane; (e) scattering in the diffusion limit, reflective backing, 50% light absorption in bulk; (f) scattering in the diffusion limit, black backing, no bulk absorption. (Adapted from Swank, 1973b.)

is that when plotted on log–log coordinate scales, the MTF consists essentially of two straight-line sections that blend into each other. The turnover frequency at which the two straight-line portions intersect is perhaps surprisingly low. The turnover frequencies are seen to vary over a range of $(0.08/d_s) < \eta < (0.3/d_s)$. Note that a turnover frequency of $1/d_s$ corresponds to one cycle per phosphor thickness. Thus a screen will always smooth out detail in an x-ray image if the size of the detail is less than a few screen thicknesses.

5.3.8 Experimental Screen MTFs and LSFs

It has been shown by Burgess (1978) that the following empirical equation provides an excellent fit to experimental results over a wide range of frequencies:

$$\mathrm{MTF}(\xi) = 0.5\,\mathrm{erfc}[\alpha \ln(\xi/\xi_0)]. \tag{5.138}$$

The complementary error function erfc( ) is defined by

$$\mathrm{erfc}(x) = \frac{2}{\sqrt{\pi}} \int_x^\infty \exp(-t^2)\,dt. \tag{5.139}$$

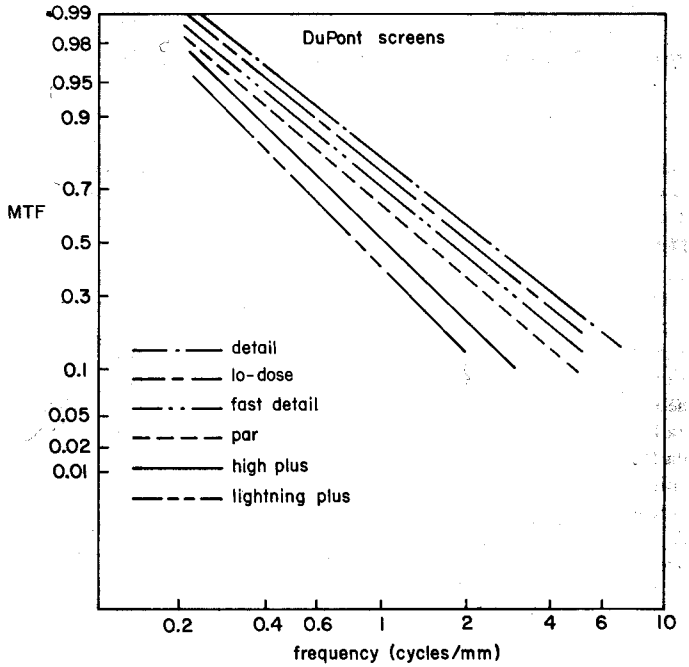

Fig. 5.33 MTF data for six DuPont screens plotted on log-cumulative probability axis. Equation (5.138) describes a straight line on this plot. (Adapted from Burgess, 1978.)

The adjustable parameter ξ_0 represents the spatial frequency at which the MTF has fallen to 0.5, and parameter α is a measure of the rate at which the frequency response falls off. This empirical expression has no obvious underlying physical interpretation.

The fit can be displayed in a linear fashion if the observed MTF data are graphed with an ordinate scaled to the cumulative Gaussian probability function and abscissa scaled logarithmically. Figure 5.33 shows results plotted this way. Notice that parameter α is simply the negative slope of the lines. Table 5.5 shows the results for a wide variety of screens.

Arnold *et al.* (1976) showed that many rare-earth screens have experimentally determined LSFs that are accurately described by the expression

$$\mathrm{LSF}(x) = k_1 \exp(k_2|x|),$$

where k_1 and k_2 are constants.

With all screens it was noted by Arnold and Bjärngard (1979) that for accurate results the energy of the x radiation should be stated. For energies above the K-absorption edge, the reabsorption of the K fluorescent radiation

TABLE 5.5

Empirical Parameters ξ_0 and α Describing the MTF Characteristics of Fluorescent Screens[a]

Screen	Manufacturer	ξ_0 $(\text{mm})^{-1}$	α	SE $(\times 10^{-2})^b$	Film
Detail	DuPont	2.45	0.68	1.18	Cronex-4
Fast Detail	DuPont	1.74	0.70	1.04	Cronex-4
Par	DuPont	1.43	0.76	1.55	Cronex-4
Hi-Plus	DuPont	1.20	0.77	1.15	Cronex-4
High Speed	DuPont	0.94	0.82	0.78	Cronex-4
Lightning Plus	DuPont	0.80	0.88	2.03	Cronex-4
Lodose I	DuPont	3.99	0.76	0.77	Lodose
Lodose II	DuPont	2.73	0.75	0.61	Lodose
Quanta II	DuPont	1.15	0.78	0.64	—
Quanta III	DuPont	0.86	0.81	0.59	—
X-omatic Fine	Kodak	3.01	0.78	1.22	XG
X-omatic Reg.	Kodak	1.48	0.79	0.62	XG
Min-R	Kodak	3.86	0.84	1.27	SO-442
Industrex F-2	Kodak	3.08	0.81	0.67	SO-146
Lanex	Kodak	1.14	0.77	1.10	Ortho G
Alpha 4	3M	1.27	0.60	0.82	XD
Alpha 8	3M	0.97	0.70	0.44	XD
Radelin UD-3	U.S. Radium	1.83	0.68	0.62	Kodak RP
TA-3	U.S. Radium	1.59	0.71	0.48	Kodak RP
TF-3	U.S. Radium	1.00	0.78	0.85	Kodak RP
STF-3	U.S. Radium	0.90	0.81	0.62	Kodak RP
Rarex BG Detail	U.S. Radium	2.07	0.67	1.04	Kodak RP
BG Mid	U.S. Radium	1.22	0.76	0.89	Kodak RP
B Mid	U.S. Radium	1.02	0.80	0.82	Kodak RP
BG High Speed	U.S. Radium	0.86	0.77	0.92	Kodak RP

[a] From Burgess (1978).

[b] Parameter SE is the standard error of the fit of the observed MTF to the empirical expression, Eq. (5.138).

within the screen has the effect of broadening the line spread function, thus degrading the resolution.

5.3.9 Relationship between Resolution and Speed

If everything is held constant except the phosphor layer thickness d_1, then speed will increase and the minimum resolvable distance will increase as d_1 increases. If we use the simple model described earlier, it is easy to determine the form of this interaction. A reasonable measure of the minimum resolvable distance is the FWHM of the line spread function δ. Using (5.135)

we find that δ is given by

$$\ln\left(\frac{(\delta/2)^2 + d_s^2}{(\delta/2)^2 + d_2^2}\right) = 0.5 \ln\left(\frac{d_s^2}{d_2^2}\right), \tag{5.140}$$

from which it follows at once that

$$\delta = 2(d_s d_2)^{1/2}. \tag{5.141}$$

This expression should be interpreted with care. As the thickness of the cover layer $d_2 \to 0$, (5.141) implies that the minimum resolvable distance $\delta \to 0$. The singular nature of (5.135) at $y = d_2 = 0$ precludes a proper definition of FWHM for this case.

The speed S of the system is directly proportional to the amount of light that is generated and that reaches the film, so with reasonable accuracy we

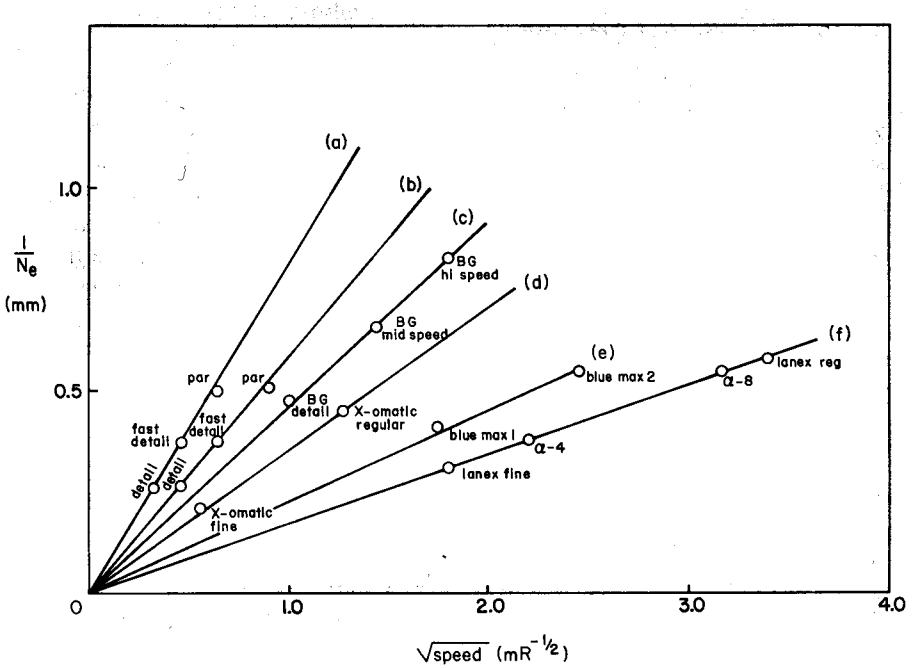

Fig. 5.34 Showing the relationship between speed and minimum resolvable distance for a variety of film–screen combinations. Provided that screens of a given composition type have the same thickness of transparent protective layer, the experimental data should be in straight lines according to Eq. (5.141). The ordinate is scaled in terms of an (equivalent pass band)$^{-1}$. This quantity is directly proportional to δ, the minimum resolvable distance defined in the text. The letters refer to the following film-screen combinations: (a) screen: DuPont $CaWO_4$; film: Kodak XG; (b) DuPont $CaWO_4$; Kodak XRP; (c) US Radium Rarex; Kodak XRP; (d) Kodak $BaSrSO_4$; Kodak XRP; (e) General Electric LaOBr; Kodak XS; (f) Kodak and 3M rare earth; 3M XM. (Adapted from Rao and Fatouros, 1978.)

can write

$$S = kd_1, \tag{5.142}$$

where k is a constant and we are still assuming that $\mu d_1 \ll 1$. By combining these last two equations and making the assumption that $d_1 \gg d_2$, we find that

$$S = \frac{k}{d_2}\left(\frac{\delta}{2}\right)^2, \tag{5.143}$$

which is the relationship between minimum resolvable distance and screen speed. This relationship was tested experimentally by Rao and Fatouros (1978) and found to hold over a wide range of screen and film types (see Fig. 5.34).